

Reaction of Zn^+ with NO_2 . The gas-phase thermochemistry of ZnO

D. E. Clemmer, N. F. Dalleska, and P. B. Armentrout

Citation: *The Journal of Chemical Physics* **95**, 7263 (1991); doi: 10.1063/1.461403

View online: <http://dx.doi.org/10.1063/1.461403>

View Table of Contents: <http://scitation.aip.org/content/aip/journal/jcp/95/10?ver=pdfcov>

Published by the AIP Publishing

Articles you may be interested in

Guided ion beam and theoretical studies of the reaction of Ag^+ with CS_2 : Gas-phase thermochemistry of AgS^+ and AgCS^+ and insight into spin-forbidden reactions

J. Chem. Phys. **132**, 024306 (2010); 10.1063/1.3285837

Unusual products observed in gas-phase $\text{W}^+ + \text{O}_2$ and D_2O reactions

J. Chem. Phys. **130**, 124314 (2009); 10.1063/1.3096414

The gas-phase thermochemistry of TiH

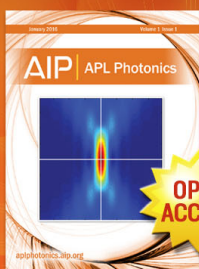
J. Chem. Phys. **95**, 1228 (1991); 10.1063/1.461154

The gas-phase thermochemistry of FeH

J. Chem. Phys. **94**, 2262 (1991); 10.1063/1.459897

Quantitative ESR Measurements of Gas-Phase H and OH Concentrations in the $\text{H}-\text{NO}_2$ Reaction

J. Chem. Phys. **43**, 1550 (1965); 10.1063/1.1696969



Launching in 2016!

The future of applied photonics research is here

AIP | APL
Photonics

Reaction of Zn^+ with NO_2 . The gas-phase thermochemistry of ZnO

D. E. Clemmer, N. F. Dalleska, and P. B. Armentrout^{a)}

Department of Chemistry, University of Utah, Salt Lake City, Utah 84112

(Received 24 June 1991; accepted 2 August 1991)

The homolytic bond dissociation energies of ZnO and ZnO^+ have been determined by using guided ion-beam mass spectrometry to measure the kinetic-energy dependence of the endothermic reactions of Zn^+ with nitrogen dioxide. The data are interpreted to yield the bond energy for ZnO , $D_0^\circ = 1.61 \pm 0.04$ eV, a value considerably lower than previous experimental values, but in much better agreement with theoretical calculations. We also obtain $D_0^\circ(\text{ZnO}^+) = 1.67 \pm 0.05$ eV, in good agreement with previous results. Other thermochemistry derived in this study is $D_0^\circ(\text{Zn}^+ - \text{NO}) = 0.79 \pm 0.10$ eV and the ionization energies, $\text{IE}(\text{ZnO}) = 9.34 \pm 0.02$ eV and $\text{IE}(\text{NO}_2) = 9.57 \pm 0.04$ eV.

INTRODUCTION

In a recent paper on the thermochemistry of gas-phase transition-metal oxide neutral and ionic diatoms,¹ we noted that there is little information about the gas-phase thermochemistry of zinc oxide. Zinc is the only first-row transition metal for which there have been no definitive measurements made of the neutral oxide bond energy, $D^\circ(\text{ZnO})$, and ionization energy, $\text{IE}(\text{ZnO})$. In 1964, Anthrop and Searcy² attempted to study this molecule by high-temperature mass spectrometry, but did not detect "gaseous zinc oxide molecules of any kind." Based on estimates of their experimental sensitivity, they assigned an upper limit for the zinc oxide bond energy of $D_{298}^\circ(\text{ZnO}) \leq 2.86$ eV. This same data was reevaluated in 1983 by Pedley and Marshall in their compilation on gaseous monoxides and they cite $D_0^\circ(\text{ZnO}) < 2.77 \pm 0.43$ eV.³ In this same year, a lower limit of $D^\circ(\text{ZnO}) \geq 2.8 \pm 0.2$ eV was obtained by Wicke, who monitored the chemiluminescent reaction of zinc atoms with N_2O as a function of kinetic energy.⁴ Wicke goes on to suggest that his lower limit, along with the upper limit of Anthrop and Searcy gives $D^\circ(\text{ZnO}) \approx 2.8$ eV. However, this value is well above the theoretical values of $D_e = 1.20, 0.66$, and 1.44 eV calculated by Bauschlicher and Langhoff,⁵ Dolg *et al.*,⁶ and Igel-Mann and Stoll,⁷ respectively. Bauschlicher and Langhoff commented on this large discrepancy but were unable to reconcile the difference.

In this paper, we report the first direct measurement of the bond energy and IE of the neutral ZnO molecule. This is achieved by using guided ion-beam techniques to characterize the kinetic-energy dependence of the reaction of Zn^+ with NO_2 . In addition, we also measure the bond energy for ionic zinc oxide, and compare this with a value previously measured from reaction of $\text{Zn}^+ + \text{O}_2$, $D_0^\circ(\text{ZnO}^+) = 1.65 \pm 0.12$ eV.¹ Further, since both the ionic and neutral zinc oxide molecules are formed in the present reaction system, the energetic difference between these reaction pathways allows a direct measurement of $\text{IE}(\text{ZnO})$.

The measurement of neutral metal-ligand thermochemistry from the reactions of metal ions is accomplished by studying the endothermic transfer of a negatively charged ligand to the metal, reaction (1):



This type of reaction has been used previously to obtain neutral metal-hydride,⁸⁻¹⁵ -methyl,^{9,10,12,16} and -oxide^{12,17,18} bond energies. Since metal-containing species such as ML have fairly low IEs, a competing process is reaction (2). Successful observation of reaction (1) therefore requires that the X fragment have a relatively low IE. The $\text{Zn}^+ + \text{NO}_2$ system, where reaction (1) leads to formation of $\text{ZnO} + \text{NO}^+$, is chosen for the present study because $\text{IE}(\text{NO}) = 9.264\,36 \pm 0.000\,06$ eV,¹⁹ much lower than the IEs of fragments of other small oxygen-containing molecules such as O_2 , CO_2 , alcohols, ketones, and aldehydes.

EXPERIMENTAL SECTION

General

Complete descriptions of the apparatus and experimental procedures are given elsewhere.²⁰ Zn^+ production is described below. The ions are extracted from the source, accelerated, and focused into a magnetic sector momentum analyzer for mass analysis. Mass-selected ions are slowed to a desired kinetic energy and focused into an octopole ion guide that radially traps the ions. The octopole passes through a static gas cell containing the neutral reactant at pressures sufficiently low (~ 0.05 – 0.13 mTorr) that multiple ion-molecule collisions are improbable. After exiting the gas cell, product and unreacted beam ions drift to the end of the octopole where they are directed into a quadrupole mass filter for mass analysis and then detected. Ion intensities are converted to absolute cross sections as described previously.²⁰ Absolute uncertainties in cross sections are generally about $\pm 20\%$. Relative uncertainties are much smaller. All product cross sections reported are the result of single ion-molecule collisions as verified by examining the pressure dependence of the product intensities.

Laboratory ion energies are related to center-of-mass (CM) frame energies by $E_{\text{CM}} = E_{\text{lab}} m/(M + m)$ where M

^{a)} Camille and Henry Dreyfus Teacher-Scholar, 1987–1992.

and m are the ion and neutral reactant masses, respectively. Sharp features in the observed cross sections are broadened by two effects: the thermal motion of the neutral gas, which has a width of $\sim 0.41 E_{\text{CM}}^{1/2}$ for these reactions,²¹ and the distribution of ion energies. The zero of the absolute energy scale and the ion energy distribution (full width at half maximum ≈ 0.4 eV lab) are measured by a retarding potential technique described elsewhere.²⁰ The uncertainty in the absolute energy scale is ± 0.05 eV lab.

Ion sources

Zn^+ used in these experiments has been produced by two sources: electron-impact ionization of zinc metal vapor and argon-ion impact on a zinc metal surface. The electron-impact source, described in detail previously,¹⁶ uses a resistively heated oven to vaporize zinc powder. The resulting zinc atoms are ionized by electron impact at electron energies between 10 and 14 eV. Ionization of Zn with electrons having energy less than 14 eV ensures that Zn^+ is produced in its electronic 2S ground state since the ionization energy of Zn is 9.394 eV and the first excited state of Zn^+ lies 6.01 eV higher in energy.²² The second source is a flow-tube source²³ that uses a dc discharge²⁴ in a 10% Ar in He flow to sputter a zinc metal surface and create zinc ions. Both sources yield similar results indicating that only ground-state Zn^+ (2S) is formed.

NO_2 purification

Nitrogen dioxide as obtained from Matheson in 99.5% purity was subjected to multiple freeze-pump-thaw cycles using liquid nitrogen. During the first freeze cycle, the solid phase (N_2O_4) was always a blue-green color indicating that N_2O_3 was also present. Before thawing, an excess of oxygen gas (roughly 10–20 times more than the initial NO_2 added) was introduced to the system. The frozen nitrogen oxides were allowed to warm up in the excess of oxygen such that any NO formed from decomposition of N_2O_3 reacted with oxygen to form NO_2 . Upon refreezing the resulting NO_2 and oxygen mixture, the resulting solid phase was always a white powder with a slight yellow tint (indicating that N_2O_4 was the main species). The excess oxygen was pumped away while the N_2O_4 was held at liquid-nitrogen temperatures. Pressures in the bulb were kept below ~ 50 Torr, in order to favor NO_2 in the $2\text{NO}_2 \rightleftharpoons \text{N}_2\text{O}_4$ equilibrium.

Results for the reaction of Zn^+ with unpurified NO_2 were drastically different than the data obtained with the purified gas. The main difference was the observation of large amounts of NO^+ formed in an exothermic process and small amounts of NO_2^+ formed exothermically. Since $\text{IE}(\text{NO}) < \text{IE}(\text{Zn})$, we believe that the exothermic behavior in the NO^+ cross section is probably due to charge transfer of Zn^+ with an NO contaminant. The origins of the exothermic formation of NO_2^+ are less clear. After purification, the exothermic behavior in both the NO^+ and NO_2^+ channels was negligible.

Thermochemical analyses

Theory^{25,26} and experiment^{27–30} show that cross sections for endothermic reactions can be modeled by Eq. (3),

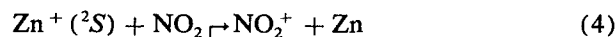
$$\sigma(E) = \sigma_0 \sum_i g_i (E - E_0 + E_i + E_{\text{rot}})^n / E, \quad (3)$$

which involves an explicit sum of the contributions of individual reactant states, denoted by i , weighted by their populations, g_i . Here, σ_0 is a scaling factor, E is the relative kinetic energy, n is an adjustable parameter, and E_0 is the 0 K threshold for reaction of the lowest electronic level of the ion with the lowest (0,0,0) vibrational level of NO_2 . E_i represents the vibrational levels of NO_2 populated at 305 K (the nominal temperature of the octopole) as calculated by a Maxwell-Boltzmann distribution^{24,31,32} and E_{rot} is the rotational energy of the neutral reagent, which for room temperature NO_2 is $3kT/2 = 0.039$ eV. Before comparison with the experimental data, this model is convoluted with the neutral and ion kinetic-energy distributions as described previously.²⁰ The σ_0 , n , and E_0 parameters are then optimized by using a nonlinear least-squares analysis to give the best reproduction of the data. Error limits for E_0 are calculated from the range of threshold values obtained for seven different data sets with different values of n and the error in the absolute energy scale.³³

In order to model some data channels, we also use a modified form of Eq. (3) which accounts for a decline in the product ion cross section at higher kinetic energies. This model has been described in detail previously,³⁴ and depends on E_D , the energy at which a dissociation channel or a competing reaction can begin, and p , a parameter similar to n in Eq. (3).

RESULTS

Four products, formed in reactions (4)–(7),



are observed from the reaction of $\text{Zn}^+ (^2S)$ with NO_2 . Figure 1 shows the cross sections for these processes as a function of kinetic energy.³⁵ All processes have cross sections that exhibit thresholds, suggesting that they are all endothermic, which immediately establishes several thermodynamic relationships: $\text{IE}(\text{NO}_2) > \text{IE}(\text{Zn})$, $D^0(\text{NO}^+ - \text{O}^-) > D^0(\text{Zn}^+ - \text{O}^-)$ (the heterolytic bond dissociation energies), and $D^0_0(\text{NO}-\text{O}) > D^0(\text{Zn}^+ - \text{O})$ and $D^0(\text{Zn}^+ - \text{NO})$ (the homolytic bond dissociation energies). Analysis of the threshold regions of these cross sections is discussed in detail below and will more precisely define these thermodynamic relationships.

At low energies, the charge-transfer process, reaction (4), dominates the reactivity. This process is near thermoneutral since the onset of the NO_2^+ cross section is only slightly above 0.0 eV (Fig. 1). The cross section for reaction (4), $\sigma(\text{NO}_2^+)$, reaches a maximum near 1.0 eV and then declines. This behavior cannot be explained by decomposition of the NO_2^+ ion since this process requires at least 2.79 eV $= D^0(\text{NO}^+ - \text{O})$, as calculated from the literature thermochemistry in Table I. Instead, the decline in $\sigma(\text{NO}_2^+)$ is

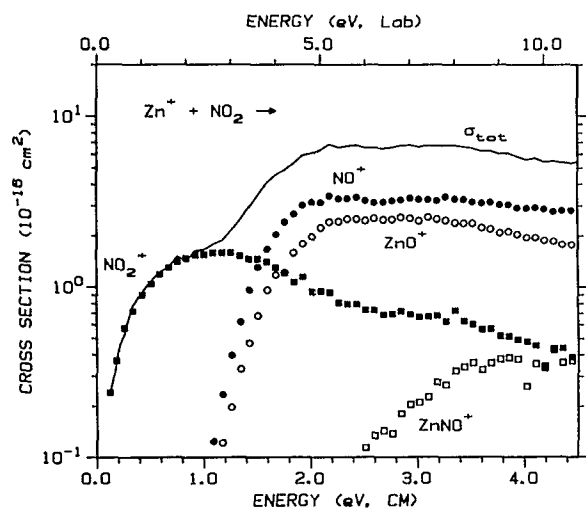


FIG. 1. Variation of product cross sections for reaction of Zn^+ with NO_2 as a function of translational energy in the center-of-mass frame (lower scale) and the laboratory frame (upper scale). Results are shown for NO_2^+ (solid squares), NO^+ (solid circles), ZnO^+ (open circles), and ZnNO^+ (open squares). The solid line represents the total reaction cross section. The data shown are the average of several independent data files.

probably due to competition with reactions (5) and (6), since the peak in $\sigma(\text{NO}_2^+)$ occurs near the onsets for these reaction channels (Fig. 1). The total reaction cross section increases substantially at the thresholds for reactions (5) and (6), indicating that these two reaction channels are more facile than reaction (4) even though the latter process is more energetically favorable by about 1 eV.

The apparent threshold for $\sigma(\text{NO}^+)$ at about 1 eV indicates that NO^+ formation must be accompanied by production of the neutral ZnO species since formation

TABLE II. Parameters of Eq. (3) used to analyze reaction cross sections.^a

Product	E_0 (eV)	σ_0	n	E_D
NO_2^+	0.18(0.04)	1.8(0.3)	1.3(0.1)	1.2(0.1)
ZnO^+	1.45(0.05)	6.4(1.4)	1.0(0.1)	
NO^+	1.38(0.04)	10.5(5.3)	1.0(0.2)	
ZnNO^+	2.33(0.10)	1.0(0.2)	1.0(0.3)	

^a Uncertainties in parentheses.

of $\text{NO}^+ + \text{Zn} + \text{O}$ cannot begin until 2.99 eV = $D^0(\text{NO}-\text{O}) + \text{IE}(\text{NO}) - \text{IE}(\text{Zn})$ (Table I). Likewise, ZnO^+ formation must be accompanied by formation of NO since production of $\text{ZnO}^+ + \text{N} + \text{O}$ would require 8.0 ± 0.1 eV (Table I). Since the $\text{ZnO} + \text{NO}^+$ and $\text{ZnO}^+ + \text{NO}$ products differ only in the location of the charge, these reaction channels must compete directly, as confirmed by the similar energy dependence of these cross sections throughout the energy range examined. Further, the similar thresholds of reactions (5) and (6) mean that $\text{IE}(\text{ZnO}) \approx \text{IE}(\text{NO})$.

THERMOCHEMISTRY

If there are no energy barriers in excess of the reaction endothermicity, as is generally the case for endothermic ion-molecule reactions,^{30,36} then the observed thresholds for reactions (4)–(7) can be used to derive thermochemistry for the product species. This assumption can be tested in the present system since literature information on reactions (4) and (5) is available for comparison. For all four reactions, the optimized fitting parameters of Eq. (3) are given in Table II.

Reaction (4), charge transfer between Zn and NO_2 , has a thermodynamic threshold that corresponds simply to the

TABLE I. Literature thermochemistry at 0 K (eV).^a

M	$\Delta_f H^0(\text{M})$	IE	$\Delta_f H^0(\text{M}^+)$
NO_2	0.372(0.008)	9.586(0.003) ^b 9.57(0.04) ^d	9.958(0.008) ^c
NO	0.930(0.002)	9.264 36(0.000 06) ^c	10.195(0.002) ^c
N^-	4.880(0.001)		
O^-	1.097(0.001)	1.461 122	2.558(0.001)
Zn	1.346(0.002)	9.394 20(0.000 02) ^f	10.740(0.002) ^c
ZnO	> 1.13(0.43) ^g < 1.1(0.2) ^h		
	2.29(0.04) ^d	9.34(0.02) ^d	11.65(0.12) ⁱ 11.63(0.05) ^d

^a Values taken from Ref. 32 unless noted otherwise. Uncertainties in parentheses.

^b Reference 40.

^c Calculated from $\Delta_f H^0(\text{M}^+) = \Delta_f H^0(\text{M}) + \text{IE}(\text{M})$.

^d This study.

^e Reference 19.

^f C. M. Brown, S. G. Tilford, and M. L. Ginter, J. Opt. Soc. Am. **65**, 1404 (1975).

^g Reference 3.

^h Reference 4.

ⁱ Reference 1.

difference in ionization energies of these two species. The accepted value for $\text{IE}(\text{NO}_2)$ has a checkered past due to unfavorable Franck-Condon factors for ionization of the neutral. Since additional experiments designed to remove the uncertainties in $\text{IE}(\text{NO}_2)$ are in progress,³⁷ we only briefly discuss the results for the Zn system here. Figure 2 displays the low-energy region of $\sigma(\text{NO}_2^+)$ and the model of Eq. (3) which uses the optimized fitting parameters given in Table II. By adding the threshold of $E_0 = 0.18 \pm 0.04$ eV to $\text{IE}(\text{Zn})$, we obtain $\text{IE}(\text{NO}_2) = 9.57 \pm 0.04$ eV. This value disagrees with most literature values,^{19,37} but agrees with limits established by Fehsenfeld, Ferguson, and Mosesman³⁸ and Killgoar *et al.*³⁹ and is in excellent agreement with a recent value of 9.586 ± 0.003 eV obtained by three-color three-photon ionization of NO_2 .⁴⁰ This agreement helps confirm this recent IE value and indicates that there are no barriers in excess of the endothermicity for process (4).

Figure 3 shows the threshold region of $\sigma(\text{ZnO}^+)$ and the best representation of the data as modeled by Eq. (3) and the parameters in Table II. By subtracting the threshold value for reaction (5) from $D_0^0(\text{ON-O}) = 3.116 \pm 0.008$ eV (Table I), we obtain $D_0^0(\text{ZnO}^+) = 1.67 \pm 0.05$ eV. This is in excellent agreement with the 1.65 ± 0.12 eV value obtained from the reaction of Zn^+ with O_2 ,¹ indicating that, as for reaction (4), there are no barriers in excess of the reaction endothermicity for process (5). This observation demonstrates that competition between reactions (4) and (5) does not influence the thermochemical measurements associated with ZnO^+ .

Figure 3 also shows the threshold region of $\sigma(\text{NO}^+)$. As for the other data channels, $\sigma(\text{NO}^+)$ is accurately represented in the threshold region by the Eq. (3) model (Table

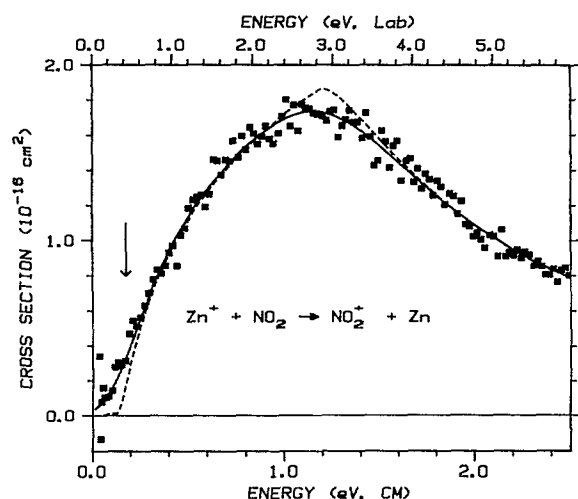


FIG. 2. Cross section for formation of NO_2^+ as a function of kinetic energy in the center-of-mass frame (lower axis) and laboratory frame (upper axis) in the threshold region. The solid line is Eq. (3) with the parameters in Table II convoluted over the experimental kinetic-energy distribution, while the dashed line is the unconvoluted model. The arrow at 0.18 eV shows the threshold for reaction (4).

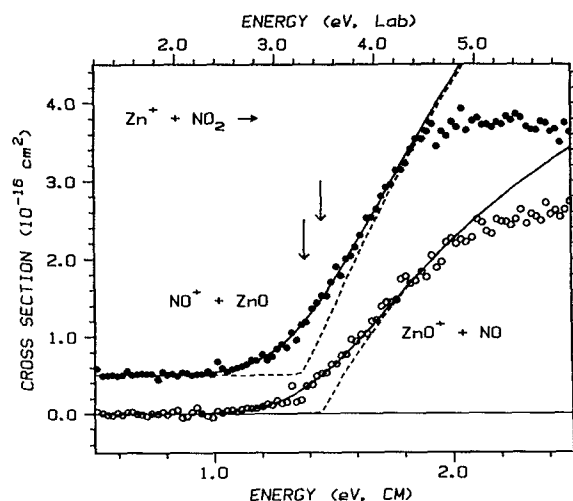


FIG. 3. Cross sections for formation of ZnO^+ and NO^+ (offset by 0.5 \AA^2) as a function of kinetic energy in the center-of-mass frame (lower axis) and laboratory frame (upper scale). The solid lines are Eq. (3) with the parameters in Table II convoluted over the experimental kinetic-energy distribution, while the dashed lines are the unconvoluted models. The arrows show the thresholds for reactions (5) and (6) at 1.45 and 1.38 eV, respectively.

II). While it is possible that the threshold associated with $\sigma(\text{NO}^+)$ is influenced by competition with reactions (4) or (5), we believe this is unlikely. Since the shapes and magnitudes of the ZnO^+ and NO^+ cross sections are similar, we expect that any competition with reaction (4) would be exhibited for both reactions (5) and (6). Furthermore, previous studies indicate that if competition between reactions (1) and (2) induces a shift in threshold, it is the process with the higher threshold that is affected.^{10,13} As noted above, the threshold for reaction (5) occurs at the thermodynamic limit for the system and, thus, the observed threshold for reaction (6) should also occur at the thermodynamic value, which is just the difference between the heterolytic bond energies, i.e., $E_0(\text{NO}^+) = D_0^0(\text{NO}^+-\text{O}^-) - D_0^0(\text{Zn}^+-\text{O}^-)$. Combining $D_0^0(\text{NO}^+-\text{O}^-) = 10.920 \pm 0.008$ eV (Table I), with $E_0(\text{NO}^+) = 1.38 \pm 0.04$ eV (Table II), yields $D_0^0(\text{Zn}^+-\text{O}^-) = 9.54 \pm 0.04$ eV. This heterolytic bond energy is related to the homolytic bond energy, $D_0^0(\text{ZnO})$, according to

$$D_0^0(\text{ZnO}) = D_0^0(\text{Zn}^+-\text{O}^-) - \text{IE}(\text{Zn}) + \text{IE}(\text{O}^-). \quad (8)$$

Use of this equation and the literature thermochemistry in Table I yields a value of $D_0^0(\text{ZnO}) = 1.61 \pm 0.04$ eV.

The ionization energy of ZnO can be determined by combining the thermochemistry for ZnO and ZnO^+ as shown by

$$\text{IE}(\text{ZnO}) = D_0^0(\text{ZnO}) + \text{IE}(\text{Zn}) - D_0^0(\text{ZnO}^+). \quad (9)$$

This procedure yields $\text{IE}(\text{ZnO}) = 9.33 \pm 0.06$ eV. A more direct and precise method of obtaining $\text{IE}(\text{ZnO})$ from our data is to measure the relative thresholds for reactions (5) and (6), since these are unaffected by any systematic errors associated with determining *absolute* thresholds.

The average difference in these thresholds, $\Delta E_0 = E_0(\text{ZnO}^+) - E_0(\text{NO}^+)$, is determined to be 0.07 ± 0.02 eV. Since $\Delta E_0 = \text{IE}(\text{ZnO}) - \text{IE}(\text{NO})$, we find that $\text{IE}(\text{ZnO}) = 9.34 \pm 0.02$ eV.

Analysis of the ZnNO^+ cross section with Eq. (3) yields the optimized fitting parameters given in Table II. Combining the threshold of $E_0 = 2.33 \pm 0.10$ eV with $D_0^0(\text{ON-O})$ leads to $D_0^0(\text{Zn}^+-\text{NO}) = 0.79 \pm 0.10$ eV; however, since $\text{IE}(\text{NO}) < \text{IE}(\text{Zn})$ (Table I), this bond energy may also be thought of as $D_0^0(\text{Zn-NO}^+) = 0.66 \pm 0.10$ eV.

DISCUSSION

While the values for $\text{IE}(\text{NO}_2)$ and $D_0^0(\text{ZnO}^+)$ obtained in this study are consistent with literature thermochemistry, the value obtained here for $D^0(\text{ZnO})$ is considerably smaller than the previous experimental determinations of approximately 2.8 eV.²⁻⁴ It is, however, in much better agreement with the theoretical D_e values of 1.20,⁵ 0.66,⁶ and 1.44 eV.⁷ These values can be converted to 0 K bond energies of 1.16, 0.62, and 1.40 eV, respectively, by using a vibrational frequency of 646 cm^{-1} .^{5,6} Our bond energy is somewhat greater than the calculated values, but this is reasonable since Bauschlicher and Langhoff⁵ note that their calculations should slightly underestimate the bond energy due to basis-set saturation, correlation, and relativistic effects, and Dolg *et al.*⁶ suggest that their value is substantially low due to insufficient treatment of electron correlation. It seems highly unlikely that the calculated values differ from the true bond energy by a factor of 2 or more since such calculations have been shown to yield quite accurate results. For example, Bauschlicher and Langhoff also calculate $D_0^0(\text{CuO}) = 2.79$ eV,⁴¹ in excellent agreement with the experimental value $D_0^0(\text{CuO}) = 2.75 \pm 0.22$ eV.³ The CuO result can also help verify the accuracy of the present experimental method since preliminary results from our laboratory on the reaction of Cu^+ with NO_2 find that $D_0^0(\text{CuO}) = 2.85 \pm 0.15$ eV.¹⁸

To further assure that the present value is correct, we can also consider the bonding in ZnO by comparing this species to other simple molecules containing zinc. The bond energies for the zinc hydride and zinc methyl molecules are well established, $D^0(\text{ZnH}) = 0.87 \pm 0.04$ eV (Ref. 42) and $D^0(\text{Zn-CH}_3) = 0.84 \pm 0.14$ eV.¹⁶ These bond energies are the lowest of all first-row transition-metal hydride and methyl molecules,^{9,43} a result that is easily rationalized by noting that the 4s and 3d orbitals of neutral Zn ($4s^2 3d^{10}$) are already fully occupied. Therefore, bonding to Zn requires promotion of a 4s electron to a 4p orbital. For similar reasons, it seems probable that the ZnO bond energy should be lower than those of other first-row transition-metal oxides,¹ consistent with our value of $D^0(\text{ZnO}) = 1.61 \pm 0.04$ eV, but not with a value of 2.8 eV.

The observation that $D^0(\text{ZnO})$ is somewhat stronger than $D^0(\text{ZnH})$ and $D^0(\text{ZnCH}_3)$ can be attributed to the relatively ionic nature of ZnO compared with ZnH and ZnCH₃. This is because oxygen has a higher electron affinity than H or CH₃.¹⁹ Indeed, Bauschlicher and Langhoff have calculated that at the equilibrium bond distance of ZnO, an

average of ~ 0.7 electrons are transferred from the zinc atom to the oxygen atom.⁵ When ZnO is ionized, an antibonding 4π electron is removed¹ [this is largely an electron centered on the oxygen atom but can be thought of as the promoted Zn(4p) electron that was donated to O in the ionic bonding picture]. Since Zn^+ is a much poorer electron donor than Zn, the extent of ionic bonding in ZnO^+ should be substantially reduced from that in ZnO; however, $\text{Zn}^+(4s^1 3d^{10})$ no longer needs to promote an electron in order to form a strong covalent bond. These two effects apparently cancel one another such that the bond energies of ZnO and ZnO^+ are similar. Theoretical calculations on this problem would be of interest.

In light of this discussion, it is also useful to consider the bonding in the ZnNO^+ molecule. One might expect the ZnNO^+ molecule to have a covalent bond formed by interaction of the 4s electron on Zn^+ and the unpaired π^* electron on NO. This bonding scheme predicts the Zn^+-NO bond energy to be similar to $D^0(\text{Zn}^+-\text{H}) = 2.36 \pm 0.13$ eV and $D^0(\text{Zn}^+-\text{CH}_3) = 3.06 \pm 0.14$ eV,¹⁶ since these species have strong single covalent bonds, as discussed previously.^{16,43} An alternative way of viewing the bonding in this molecule notes that $\text{IE}(\text{NO}) < \text{IE}(\text{Zn})$, such that the lowest-energy dissociation pathway for ZnNO^+ is to $\text{Zn}(^1\text{S}) + \text{NO}^+(^1\Sigma^+)$. Thus, the bonding between these two closed-shell species may be largely electrostatic. The relatively weak bond energy, $D_0^0(\text{Zn-NO}^+) = 0.66 \pm 0.10$ eV, suggests that the latter bonding scheme may be more accurate. Theoretical calculations on such species would be of interest in clarifying this situation.

Comparison with previous results

Assuming that our value for $D^0(\text{ZnO})$ is correct, it is of interest to reassess the previous experimental results in order to explain the apparent discrepancies. Since Anthrop and Searcy² did not actually observe any zinc oxide molecules, the present result is completely consistent with their derived upper limit for $D^0(\text{ZnO})$. The origins of the discrepancy with Wicke's⁴ lower limit of 2.8 ± 0.2 eV are less evident. There are no obvious problems in the interpretation of Wicke's data, although his threshold analysis hinges on a relatively weak tail in his chemiluminescence data. If we use our bond energy for ZnO, we calculate that he should have observed a kinetic-energy threshold for chemiluminescence near 2.2 eV. In fact, this is approximately the energy where the chemiluminescence data begins to rise above the Arrhenius model used by Wicke to fit his threshold data. This implies that the weak chemiluminescent tail does not correspond to the reaction of ground-state Zn with N_2O to form ground-state ZnO.

One possible explanation for a kinetic-energy onset to chemiluminescence that is too low is the presence of excited-state Zn. Wicke considered this and estimated that the zinc beam used in his experiment has less than 0.1% excited-state Zn atoms, suggesting that the reactivity observed is mainly due to reaction of ground-state atoms. However, the weak tail at low kinetic energies could still be explained if the reaction efficiency of this small percentage of excited states was

much higher than that of ground-state zinc. Since the ground state of Zn is a 1S closed shell, while the excited states are open-shell species, this seems quite plausible. Differences in electronic state reactivity of 1–3 orders of magnitude have been documented in the reactions of transition-metal ions.⁴⁴

ACKNOWLEDGMENTS

This work is supported by the National Science Foundation, Grant No. CHE 8917980. We are also grateful to James Chou, Kevin Glaeske, and Carl Howard for advice about purifying and handling NO_2 .

- ¹ E. R. Fisher, J. L. Elkind, D. E. Clemmer, R. Georgiadis, S. K. Loh, N. Aristov, L. S. Sunderlin, and P. B. Armentrout, *J. Chem. Phys.* **93**, 2676 (1990).
- ² D. F. Anthrop and A. W. Searcy, *J. Phys. Chem.* **68**, 2335 (1964).
- ³ J. B. Pedley and E. M. Marshall, *J. Phys. Chem. Ref. Data* **12**, 967 (1983).
- ⁴ B. G. Wicke, *J. Chem. Phys.* **78**, 6036 (1983).
- ⁵ C. W. Bauschlicher and S. R. Langhoff, *Chem. Phys. Lett.* **126**, 163 (1986).
- ⁶ M. Dolg, U. Wedig, H. Stoll, and H. Preuss, *J. Chem. Phys.* **86**, 2123 (1987).
- ⁷ G. Igel-Mann and H. Stoll (to be published), as cited in Ref. 6.
- ⁸ M. A. Tolbert and J. L. Beauchamp, *J. Phys. Chem.* **90**, 5015 (1986).
- ⁹ P. B. Armentrout and R. Georgiadis, *Polyhedron* **7**, 1573 (1988).
- ¹⁰ R. Georgiadis, E. R. Fisher, and P. B. Armentrout, *J. Am. Chem. Soc.* **111**, 4251 (1989).
- ¹¹ E. R. Fisher and P. B. Armentrout, *J. Phys. Chem.* **94**, 1674 (1990).
- ¹² L. S. Sunderlin and P. B. Armentrout, *J. Phys. Chem.* **94**, 3589 (1990).
- ¹³ R. H. Schultz and P. B. Armentrout, *J. Chem. Phys.* **94**, 2262 (1991).
- ¹⁴ Y.-M. Chen, D. E. Clemmer, and P. B. Armentrout, *J. Chem. Phys.* **95**, 1228 (1991).
- ¹⁵ Y.-M. Chen, D. E. Clemmer, and P. B. Armentrout (unpublished).
- ¹⁶ R. Georgiadis and P. B. Armentrout, *J. Am. Chem. Soc.* **108**, 2119 (1986).
- ¹⁷ R. Georgiadis and P. B. Armentrout, *Int. J. Mass Spectrom. Ion Processes* **89**, 227 (1989).
- ¹⁸ D. E. Clemmer, N. F. Dalleska, S. K. Loh, and P. B. Armentrout (unpublished).
- ¹⁹ S. G. Lias, J. E. Bartmess, J. F. Liebman, J. L. Holmes, R. D. Levin, and W. G. Mallard, *J. Phys. Chem. Ref. Data* **17**, Suppl. 1 (1988).
- ²⁰ K. M. Ervin and P. B. Armentrout, *J. Chem. Phys.* **83**, 166 (1985).
- ²¹ P. J. Chantry, *J. Chem. Phys.* **55**, 2746 (1971).
- ²² C. Corliss and J. Sugar, *J. Chem. Phys. Ref. Data* **11**, 135 (1982).
- ²³ For a complete description of this source see R. H. Schultz and P. B. Armentrout, *Int. J. Mass Spectrom. Ion Processes* **107**, 29 (1991).
- ²⁴ R. H. Schultz, K. C. Crellin, and P. B. Armentrout, *J. Am. Chem. Soc.* (in press).
- ²⁵ N. Aristov and P. B. Armentrout, *J. Am. Chem. Soc.* **108**, 1806 (1986).
- ²⁶ W. J. Chesnavich and M. T. Bowers, *J. Phys. Chem.* **83**, 900 (1979).
- ²⁷ L. Sunderlin, N. Aristov, and P. B. Armentrout, *J. Am. Chem. Soc.* **109**, 78 (1987).
- ²⁸ P. B. Armentrout and J. L. Beauchamp, *J. Chem. Phys.* **74**, 2819 (1981); *J. Am. Chem. Soc.* **103**, 784 (1981).
- ²⁹ B. H. Boo and P. B. Armentrout, *J. Am. Chem. Soc.* **109**, 3549 (1987).
- ³⁰ P. B. Armentrout, in *Advances in Gas Phase Ion Chemistry, Vol. 1*, edited by N. G. Adams and L. M. Babcock (JAI, Greenwich, CT, in press).
- ³¹ Vibrational frequencies for NO_2 are 1357.8, 756.8, and 1665.5 cm^{-1} (Ref. 32).
- ³² M. W. Chase, C. A. Davies, J. R. Downey, D. J. Frurip, R. A. McDonald, and A. N. Syverud, *J. Phys. Chem. Ref. Data* **14**, Suppl. 1 (1985) (JANAF Tables).
- ³³ In the case of $\sigma(\text{ZnNO}^+)$, only five independent data sets were analyzed. Two of the seven total data sets were threshold scans that did not go to high enough energies to observe ZnNO^+ . See the Results section.
- ³⁴ M. E. Weber, J. L. Elkind, and P. B. Armentrout, *J. Chem. Phys.* **84**, 1521 (1986).
- ³⁵ The absolute magnitudes of all products but NO^+ were easily reproducible within a 20% uncertainty. The NO^+ product exhibited larger variations in magnitude consistent with product collection difficulties. This kind of behavior is typically exhibited by products that are formed with little forward momentum in the laboratory frame.
- ³⁶ P. B. Armentrout, in *Structure/Reactivity and Thermochemistry of Ions*, edited by P. Ausloos and S. G. Lias (Reidel, Dordrecht, 1987), p. 97.
- ³⁷ D. E. Clemmer and P. B. Armentrout (unpublished).
- ³⁸ F. C. Fehsenfeld, E. E. Ferguson, and M. Mosesman, *Chem. Phys. Lett.* **4**, 73 (1969).
- ³⁹ P. C. Killgoar, G. E. Leroi, W. A. Chupka, and J. Berkowitz, *J. Chem. Phys.* **59**, 1370 (1973).
- ⁴⁰ K. S. Haber, J. W. Zwanziger, F. X. Campos, R. T. Wiedmann, and E. R. Grant, *Chem. Phys. Lett.* **144**, 58 (1988).
- ⁴¹ S. R. Langhoff and C. W. Bauschlicher, *Chem. Phys. Lett.* **124**, 241 (1986). The D_0^0 value cited here is calculated from $D_e = 2.83$ eV and $\omega_e = 606$ cm^{-1} .
- ⁴² K. P. Huber and G. Herzberg, *Constants of Diatomic Molecules* (Van Nostrand, New York, 1979).
- ⁴³ P. B. Armentrout, *ACS Symp. Ser.* **428**, 18 (1990).
- ⁴⁴ P. B. Armentrout, *Annu. Rev. Phys. Chem.* **41**, 313 (1990).